Conceptual Design of *n*-Butyl Acetate Synthesis Process by Reactive Distillation Using Residue Curve Maps

Zheng, Huidong
School of Chemical Engineering, Fuzhou University, Fuzhou, 350108, Fujian, P.R. CHINA

Tian, Hui*[+]
College of Chemistry and Chemical Engineering, Yantai University, Yantai, 264005, Shandong, P.R. CHINA

Shen, Yanyi; Wang, Jie; Zhao, Suying*[+]
School of Chemical Engineering, Fuzhou University, Fuzhou, 350108, Fujian, P.R. CHINA

ABSTRACT: *Residue curve maps are a powerful tool for the preliminary design of Reactive Distillation (RD). In this study, residue curve maps of the n-butyl acetate synthesis reaction were calculated based on the Langmuir–Hinshelwood–Hougen–Watson kinetic and UNIQUAC models to calculate the physical properties of the system. The results showed that the unstable node branch emerged from the n-butyl acetate/water edge, moved toward the chemical equilibrium surface with increasing Damköhler number, and no ternary reactive azeotropic point appeared when the reaction was added. Conceptual design of n-butyl acetate synthesis by reactive distillation based on residue curve maps is presented. Based on the simulation results, both the energy consumption and the total annual cost were lower than previously reported values.*

KEYWORDS *Residue curve map; N-butyl acetate; Conceptual design; Reactive distillation.*

INTRODUCTION

n-Butyl acetate (*n*-BuAc) is a common solvent that is used in large quantities in coating manufacture, lacquers, and other processes [1, 2]. Because of its environmentally friendly characteristics and low toxicity, the consumption of *n*-BuAc has grown in the last few decades [3]. The esterification reaction using acetic acid (HAc) and *n*-butanol (*n*-BuOH) in the presence of an acidic catalyst is the most common process to produce *n*-BuAc. However, the equilibrium limitation becomes a critical issue in the production of *n*-BuAc with the reversible esterification reaction. To achieve a high conversion of *n*-BuOH and overcome the equilibrium limitation of the reversible the reaction, Reactive Distillation (RD), where the reaction and separation are simultaneously performed in one column, has become an important technique to produce *n*-BuAc. Studies of *n*-BuAc synthesis in one RD column (RDC) are plentiful in the literature. *Liao* [2] studied the process of *n*-BuAc synthesis by RD with a cation exchange resin and the conversion of HAc reached 94%. Hanika [4] investigated *n*-BuAc synthesis in a packed RDC using experimental and computational methods. The results showed that high purity (>99%) *n*-BuAc could be obtained with 50 theoretical stages by the RD process. Steinigeweg*et* [5] used the RD process to

* *To whom correspondence should be addressed.*
+ E-mail: tianhui@ytu.edu.cn ; zhaosuying@fzu.edu.cn
1021-9986/2018/3/107-115 9/$/5.09

produce *n*-BuAc in a pilot plant unit based on computer analog calculations. Both the reaction kinetics and thermodynamic experiments were investigated in a RDC with 30 theoretical stages. *Gangadwala* [6] and *Jimenexet* [7] produced methanol and *n*-BuAC from *n*-BuOH and methyl acetate. The results showed that high purity *n*-BuAc could be produced using three columns with a 43 theoretical stage RDC.

Because of the complexity of RD, most of the studies about RD processes lack a feasibility analysis. Residue Curve Maps (RCMs) are a powerful tool in the conceptual design of the RD process, and RCMs had been successfully applied in complex non-ideal RD processes. In addition, RCMs can be constructed based only on the Liquid-Liquid Equilibrium (LLE), Vapor-Liquid Equilibrium (VLE), reaction kinetics, and chemical equilibrium data [8-12]. RCMs generally have the following characteristics:

1- They have no relation to the volume of the remaining liquid, which is determined by the VLE at a known pressure.

2- RCM lines generally point to high boiling composition mixers.

3- The pathways of RCM lines do not interact with each other.

RCMs have been reported for different processes. RCMs of the propyl acetate synthesis reaction were investigated by *Huang* [11] found that the positions of singular points are influenced by different heating policies, and the reaction kinetics also control the topology of the RCMs, except when the Damköhler number *Da* = 0 or ∞. *Sanchez-Dazaet* [12] used the methodology to determine a new calculation method for RCMs based on the element concept. Using RCMs, *Almeida-Riveraet* [13] analyzed methyl *tert*-butyl ether synthesis by RD at 11 atm. *Duarteet* [14] studied the heterogeneous catalytic system using RCMs. They investigated the influences of temperature, the ratio of the vapor flow rate to the liquid holdup, and *Da* value on the adsorptive models. We have previously investigated RCMs of the ethyl acetate system [15]. *Wang* [16] studied the feasibility of conducting the transesterification of propylene glycol ether (PM) with methyl acetate (MeAc) by the Residue Curve Maps (RCM), and the results showed that full conversion of PM could be realized by RD with a mole ratio of MeAc-PM larger than 2.882. Based on the residue curve maps of HCl-ethanol-water, a distillation column was designed to accomplish three design constraints by *José* [17]: HCl-water commercial product composition, maximum ethanol recovery for recycling, and minimum energetic duty in the reboiler. With the aim of saving energy and capital cost, *You* [18] through the analysis of a ternary residue curve map and is volatility curves observed that the minimal amounts of entrained feed and extractive feasible regions in the ternary diagram are sensitive to pressures.

The singular points in RCMs always contain saddle, unstable, and stable nodes along with residue curve lines, and the temperature always increases. This information makes RCMs promising for the conceptual design of RD. We found lots of works of literature using RCMs to study the feasibility of esterification reaction, hydration reaction, transesterification and so on [19-22], while we don't find the detailed study of *n*-BuAc synthesis reaction feasibility analysis. So in this study, RCMs of the *n*-BuAc synthesis reaction were constructed, and conceptual design of the RD process was carried out based on analysis of the RCMs. Finally, simulations were performed based on the conceptual design.

THEORETICAL SECTION

Model of RCMs

The reaction of *n*-BuOH with HAc is as follows:

$$\mathrm{HAc + n-BuOH \leftrightarrow H_2O + n-BuAc} \quad (1)$$

The experimental setup for the determination of RCMs by simple batch, distillation is shown in Fig. 1. To obtain the RCMs, the catalyst and mixtures with different initial liquid compositions were added to the reactor. The composition of the liquid remaining in the reactor was continuously measured when the liquid was heated to a specific temperature. The experiment was terminated when the amount of liquid residue was too small to measure. The mass balance without the simple batch distillation reaction is

$$\frac{dH}{dt} = -V \quad (2)$$

$$\frac{d(Hx_i)}{dt} = -Vy_i \quad (3)$$

$$\frac{dx_i}{dt} = \frac{V}{H}(x_i - y_i) \quad (4)$$

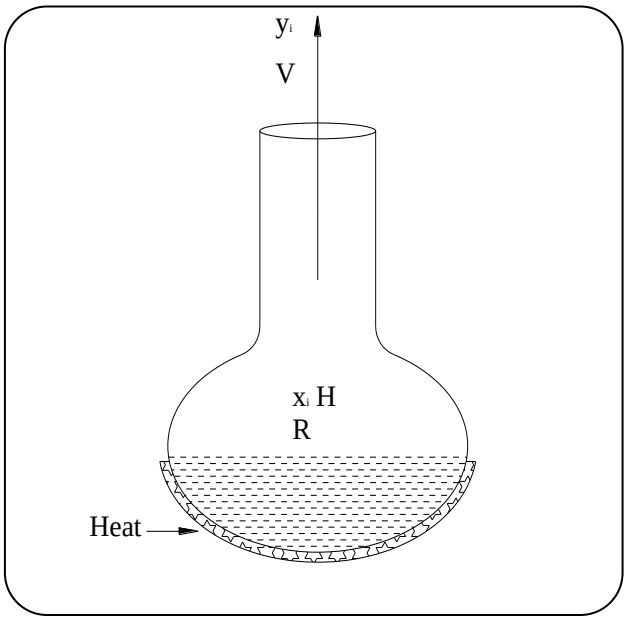

Fig. 1: Experimental setup for the determination of RCMs by simple batch distillation.

$$\frac{dx_i}{d\xi} = x_i - y_i \tag{5}$$

where $x_i(y_i)$ is the mole fraction of component i in the liquid(vapor) phase, V is the evaporation rate, H is the liquid volume in the reactor, and ξ is the dimensionless time with $d\xi = \frac{V}{H}dt$. The RCMs can be expressed as follows [14]:

$$\frac{dx_i}{d\xi} = x_i - y_i + \frac{H}{V}(\upsilon_i - \upsilon_T x_i)k_f\left(\prod_{r=1}^{c_r} a_r^{|\upsilon_r|} - \frac{1}{K}\prod_{p=1}^{c_p} a_p^{|\upsilon_p|}\right) \tag{6}$$

where υ is the stoichiometric coefficient of the added reaction, K is the equilibrium constant of the reaction, k_f is the rate constant of the forward reaction, and c_p and c_r are the amounts of products and reactants, respectively. *Da* and the dimensionless reaction rate R, which depends on the composition of the liquid phase, can be expressed as

$$R = \frac{r}{k_f} = \prod_{r=1}^{c_r} a_r^{|\upsilon_r|} - \frac{1}{K}\prod_{p=1}^{c_p} a_p^{|\upsilon_p|} \tag{7}$$

$$Da \equiv \frac{\frac{H_0}{V_0}}{\frac{1}{k_{f,\,ref}}} \tag{8}$$

Thus, Eq.(6) can be rewritten as

$$\frac{dx_i}{d\xi} = x_i - y_i + \frac{H}{V}\frac{V_0}{H_0}(\upsilon_i - \upsilon_T x_i)\frac{k_f}{k_{f,\,ref}}DaR \tag{9}$$

Where $k_{f,\,ref}$ is the reaction rate constant of the forward reaction in the reference states.

When the heating strategy obeys $V/H = V_0/H_0$ = constant and the reaction system is pseudo-homogeneous, Eq. (9) can be rewritten as

$$\frac{dx_i}{d\xi} = x_i - y_i + (\upsilon_i - \upsilon_T x_i)\frac{k_f}{k_{f,\,ref}}DaR \tag{10}$$

Equation (10) was used to calculate the RCMs of the *n*-BuAc synthesis reaction.

Kinetic model

In this study, the Langmuir–Hinshelwood–Hougen–Watson (LHHW) kinetic model was used to describe the *n*-BuAc esterification reaction. The reaction rate of the LHHW model is

$$r_{BuOH} = M_{cat}K_f K_{s,\,HAc}K_{s,\,BuOH} \times \frac{C_{HAc}C_{BuOH} - C_{BuAc}C_{H_2O}/K_a}{(1 + K_{s,\,HAc}C_{HAc} + K_{s,\,BuOH}C_{BuOH} + K_{s,\,BuAc}C_{BuAc} + K_{s,\,H_2O}C_{H_2O})^2} \tag{11}$$

where C_{BuOH}, C_{HAc}, C_{H2O}, and C_{BuAc} are the concentrations of *n*-BuOH, HAc, H_2O, and *n*-BuAc (mol/L), respectively, r is the reaction rate of *n*-BuOH (mol/s), K_f is the reaction rate constant (mol/(gs)), M_{cat} is the catalyst weight in the reaction (g),$K_a$is the chemical reaction equilibrium constant, and K_s is the adsorption equilibrium constant. All of the *K*p can be expressed as

$$K = a\exp(b/RT) \tag{12}$$

All of the parameters in the LHHW kinetic model were obtained from *Qiu* [23] using Amberlyst-36 as the catalyst, and they are shown in Table 1.

Vapor-liquid equilibrium

The vapor fraction y_i can be expressed as

$$y_i P = \gamma_i x_i P_i^{sat} \tag{13}$$

Where x_i (y_i) is the mole fraction of component i in the liquid (vapor) phase and γ_i is the activity coefficient. where p_i^{sat} is the saturated vapor pressure of component i and calculated by Antoine equation. The parameters

Table 1: Parameters of the LHHW kinetic model.

parameter	K_f	K_a	$K_{s,BuAc}$	$K_{s,HAc}$	$K_{s,BuOH}$	K_{s,H_2O}
a kmol/kg·s	1.45×10^{4}	1.23×10^{3}	2.86×10^{-3}	6.44×10^{-1}	2.84×10^{-7}	3.88×10^{-4}
b kmol/kg·s	-6.45×10^{3}	1.96×10^{3}	2.47×10^{4}	5.41×10^{3}	4.80×10^{4}	2.92×10^{4}

Table 2: Parameters of Eq.(14) [24].

Parameters / Components	*a*	*b*	*c*	*d* ×10^{-3}	*e*	*f* ×10^{-17}	*g*
n-BuOH	93.1730	-9185.9000	0	0	-9.7464	0.4780	6
HAc	30.5531	-5699.3122	0	5.4118	-0.3965	8.0651	6
n-BuAc	76.3400	-7285.8000	0	0	-6.9459	0.9989	6
H_2O	65.1544	-6842.9073	0	2.7835	-6.1364	3.3117	6

of the substances were obtained from the literature [24], and calculated by Eq.(14).

$$P_i^{sat} = \exp(a + \frac{b}{T+c} + d\times T + e\times \ln(T) + f\times T^{g}) \qquad (14)$$

The UNIQUAC model was used to calculate the liquid phase activity coefficient of the *n*-BuAc reactive system:

$$\ln\gamma_i = \ln\frac{\Phi_i}{x_i} + \frac{z}{2}q_i\ln\frac{\theta_i}{\Phi_i} - q_i'\ln t_i' - \frac{q'\sum_j \theta_j'\tau_{ij}}{t_j'} + l_i + q_i' - \frac{\Phi_i}{x_i}\sum_j x_j l_j \qquad (15)$$

where $\theta_i = \frac{q_i x_i}{q_T}$; $q_T = \sum_k q_k x_k$

$\theta_i' = \frac{q_i' x_i}{q_T'}$; $q_T' = \sum_k q_T' x_k$

$\Phi_i = \frac{r_i x_i}{r_T}$; $r_T = \sum_k r_k x_k$

$l_i = \frac{z}{2}(r_i - q_i) + 1 - r_i$; $t_i' = \sum_k \theta_k'\tau_{ki}$

$\tau_{ij} = \exp(a_{ij} + b_{ij}/T + C_{ij}\ln T + d_{ij}T)$

$z = 10$; $a_{ij} \neq a_{ji}$; $b_{ij} \neq b_{ji}$; $c_{ij} \neq c_{ji}$; $d_{ij} \neq d_{ji}$

The parameters are listed in Table 3. The compositions and the boiling temperature of the azeotropic mixtures were calculated at 1.0 atm and they are shown in Table 4.

Equilibrium constant

K_{eq} is the chemical equilibrium constant for the esterification reaction:

$$K_{eq} = \prod_{i=1}^{i=n}(\gamma_i \cdot x_i)^{\upsilon_i} = f(x_i, \gamma_i(x_i, T)) \qquad (16)$$

ANALYSIS

The Damköhler number *Da* is the most important parameter in the RCMs with a reaction. The *Da* value indicates the influence of a reaction in the RCMs, and it is the ratio of the phase equilibrium to the reactive equilibrium strength [26-27]. When the reaction achieves equilibrium and there is a balance between the reactive equilibrium and the phase equilibrium, *Da* achieves the limiting value Da_{lim}. When $Da>Da_{lim}$, it does not affect the RCMs. $Da=0$ indicates that the system has no reaction, as shown in Eq.(10). The system achieves balance when *Da* approaches Da_{lim}. The system is kinetically controlled when $0 < Da < Da_{lim}$.

The RCMs of the then-BuAc system without a reaction at 1 atm are shown in Fig. 2. Three binary azeotropes and one ternary azeotrope exist in the RCMs. The binary azeotropes H_2O/*n*-BuOH (Az.2), *n*-BuAc/H_2O (Az.3), and *n*-BuOH/*n*-BuAc (Az.4)are the saddle nodes, and the ternary azeotrope *n*-BuAc/*n*-BuOH/H_2O (Az.1) is the unstable node. The pure components *n*-BuOH, H_2O, and HAc are also saddle nodes, and *n*-BuAc is the only stable node in the reactive system. The lowest boiling point temperature is the ternary azeotrope *n*-BuAc/*n*-BuOH/H_2O at 363.8K, which is chose as the reference temperature.

Table 3: Parameters of the UNIQUACactivity coefficient model.

Component *i*	*n*-BuAc	*n*-BuAc	*n*-BuAc	*n*-BuOH	*n*-BuOH	H_2O
Component *j*	*n*-BuOH	H_2O	HAc	H_2O	HAc	HAc
a_{ij}	0	-63.4375	0	0	0	0
a_{ji}	0	-35.2359	0	0	0	0
b_{ij}	-12.39	1998.481	-358.1	9.1794	-17.83	-73.444
b_{ji}	-41.5	1854.037	150	-267.1	15.85	219.66
c_{ij}	0	9.6627	0	0	0	0
c_{ji}	0	5.0042	0	0	0	0
d_{ij}	0	0	0	0	0	0
d_{ji}	0	0	0	0	0	0

Table 4: Compositions and temperatures at1.0 atm.

Azeotrope	Data from ref [4-5, 25]				Calculated Data			
	BuOH mol.%	BuAc mol.%	H_2O mol.%	T K	BuOH mol.%	BuAc mol.%	H_2O mol.%	T K
n-BuAc-H_2O	0.00	28.87	71.13	364.3	0.00	28.30	71.70	364.07
n-BuOH-H_2O	24.76	0.00	75.24	366.1	22.05	0.00	77.95	366.92
n-BuOH- *n*-BuAc	78.73	21.27	0.00	389.3	78.5	21.50	0.00	390.05
n-BuOH- *n*-BuAc-H_2O	4.78	24.01	71.21	363.8	3.24	28.47	68.29	363.98

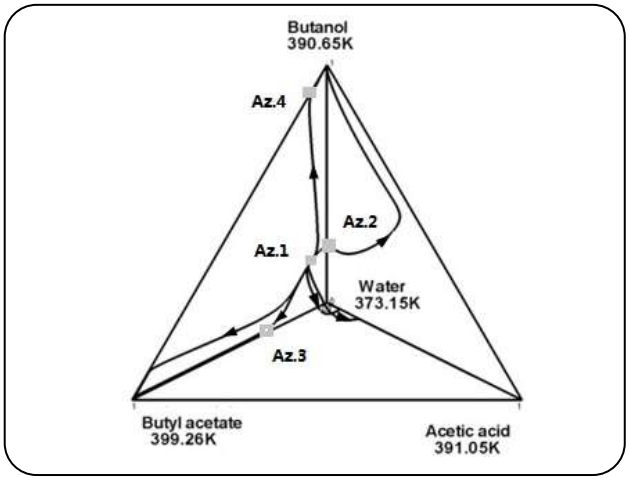

Fig. 2: RCMs with Da=0.

The RCM lines usually originate from the unstable node, approach the saddle-node, and finally converge to the stable node.

Because of the existence of four components and four azeotropes in the *n*-BuAc reaction system, it is more preferable to perform reaction distillation for better separation. So RCMs with reaction was further studied in the following section. The RCMs with the same initial compositions when $Da \neq 0$ are shown in Fig. 3(a). No reaction azeotrope appears and adding the reaction has no influence on the azeotropic compositions. The RCMs were transformed into a planar graph for better visualization (Fig. 3(b)).

CONCEPTUAL DESIGN

According to the analysis of the RCMs, the pure component *n*-BuAc has the highest boiling point (399.15K at 1 atm) in the reactive system and should be obtained at the bottom of the RDC. The boiling points of Az.1, Az.2, and Az.3 are low and close together, and they should be obtained at the top of the RDC. A high purity *n*-BuAc product (≥99.5%) cannot be obtained when only one RDC is used, because the ratio of the reactive equilibrium strength to the phase equilibrium strength achieves equilibrium when $Da \neq 0$, so another Purification Distillation Column (PDC) is added to the process design. A schematic diagram of the preliminary design to produce *n*-BuAc by RD is shown in Fig.4. *n*-BuOH and HAc are added into the RDC. After the primary reaction

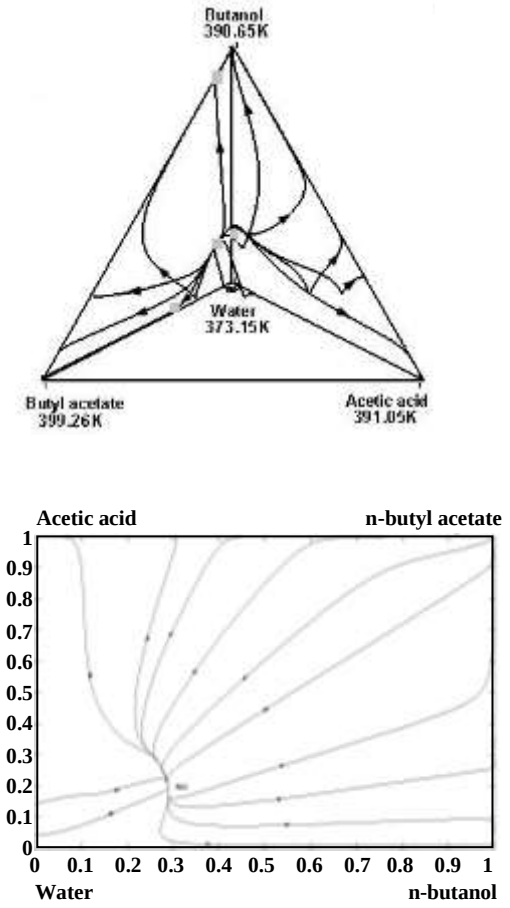

Fig. 3: (a) RCMs with Da≠0. (b) The RCMs in (a) transformed into a planar graph.

and purification, the overhead vapor products of the RDC are *n*-BuAc/H_2O/*n*-BuOH, *n*-BuAc/H_2O, and H_2O/*n*-BuOH mixtures, which could be condensed and introduced into a decanter for phase separation. The organic phase is refluxed back into the RDC and the aqueous phase is removed. The *n*-BuAc withdrew from the bottom of the RDC is fed into the PDC, and the *n*-BuAc product is obtained at the bottom of the PDC. The operating curves are shown in Fig. 5. Reflux $L_1$and feedstock F_0arefed into the RDC. After reaction and purification, a bottom product $B_1$and a top product V_1areobtained

MODELING AND SIMULATION

Modeling

RD is an extremely complex process, which includes not only the reaction but also the mass transfer process. Simulation of *n*-BuAc synthesis by RD was performed using Aspen Plus, and the flow sheet is shown in Fig.4. Based on the rigorous equilibrium stage model, the RADFRAC module in Aspen Plus was used to describe the multistage vapor-liquid separation process and the reaction in the RD column. The decrease in pressure along the column was ignored to simplify the calculation [13, 28], and the whole equipment was operated at 1 atm. The specifications of the RDC and PDC are listed in Table 5. HAc and *n*-BuOH were defined as analytical reagents. The diameters of the columns were calculated with a production capacity of *n*-BuAcof10,000tons/year with a feed molar ratio of HAc to *n*-BuOH of 1.0.

Simulation results

To compare the results with other processes, the energy consumption and the Total Annual Cost (TAC) were calculated, and the *n*-BuAc product purity was defined to be 99.5 wt.%. The simulation results showed that the energy consumption was 4680MW and the TAC was 2787693 USD/year for a production capacity of *n*-BuAc of10,000tons/year. Both energy consumption and TAC are lower than other reported values [4, 29].

CONCLUSIONS

RCMs are a powerful tool for the conceptual design of the *n*-BuAc RD process. In this study, RCMs were calculated for the *n*-BuAc esterification reaction based on the UNIQUAC activity coefficient model and the LHHW kinetic model. The rRCMs either with or without reaction were calculated. Based on the RCMs, three binary azeotropes and one ternary azeotrope exist. Adding the reaction has no influence on the azeotropic compositions and temperature. Conceptual design of *n*-BuAc synthesis by RD was carried out based on the RCMs, and a high-purity *n*-BuAc product could be obtained. Both the energy consumption and the TAC were calculated based on the simulation, and the values were both lower than previously reported values. In a word, this proposed process avoided drawbacks associated with conventional processes, and most importantly, improved the conversion and reaction rate significantly.

Nomenclature

C	Concentration, mol/L
c_p	Quantity of products
c_r	Quantity of reactants

Table 5: Specifications of the columns.

Column	PDC	RDC
Total stages	22	23
Rectifying section	2-11stages	1-7 stages
Reactive section		8-13 stages
Stripping section	12-21 stages	14-22 stages
Feed stage	12	8
Diameter/m	0.372	0.832
Liquid holdup m^3/m^3(reactive section)		0.237
Reflux ratio	1.0	

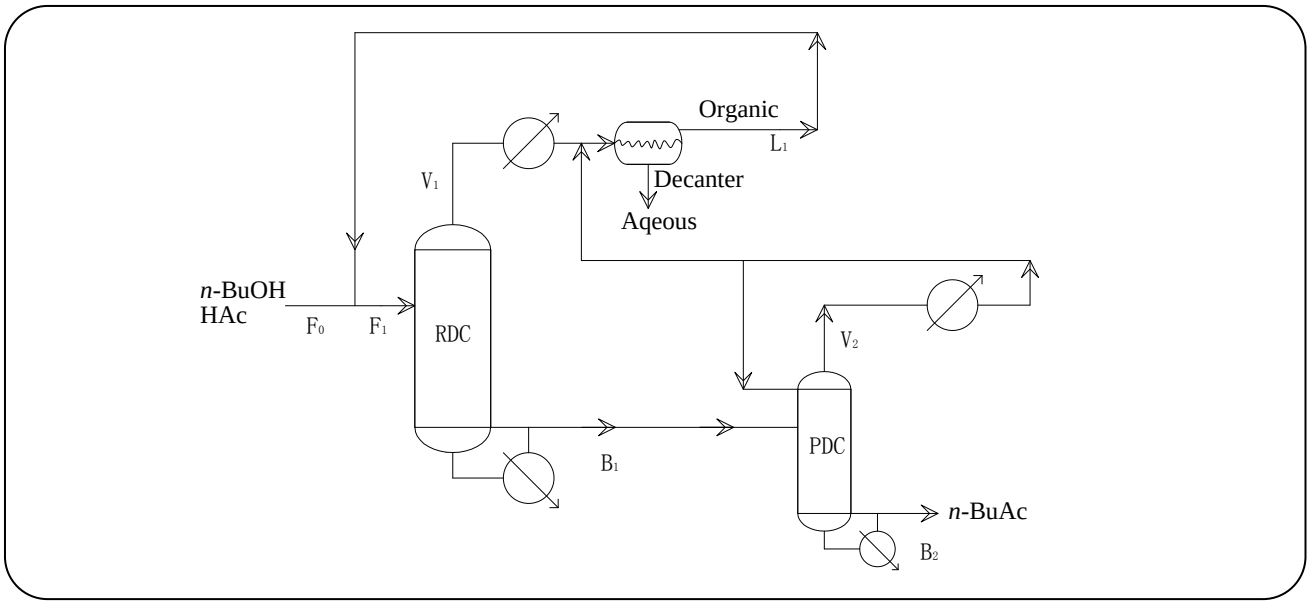

Fig. 4: Preliminary design for the production of n-BuAc by RD.

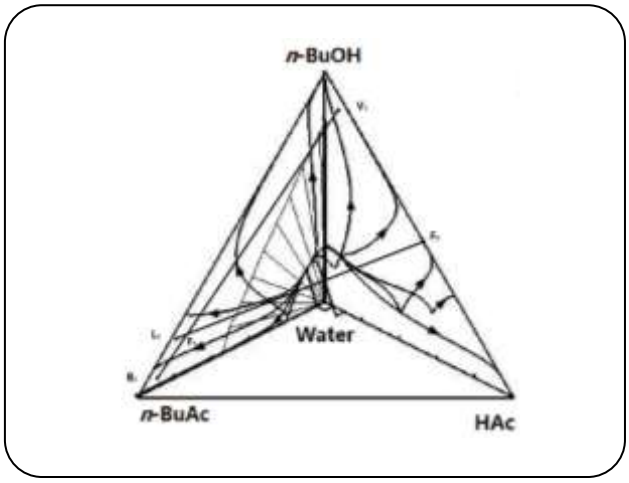

Fig. 5: Operating curves for production ofn-BuAc by RD.

Da	Damköler number
H	Liquid volume, m^3
K	Reaction equilibrium constant
K_a	Chemical reaction equilibrium constant
K_{eq}	Chemical equilibrium constant for the reaction
K_s	Adsorption equilibrium constant
k	Reaction rate constant, mol/(g·s)
K_f	Forward reaction rate constant
M_{cat}	Catalyst weight, g
P	Pressure, Pa
P_i^{sat}	Saturated pressure, Pa
R	Dimensionless reaction rate depending
R	Reaction rate, mol/s
T	Absolute temperature, K

t	Time, s
V	Evaporation rate, mol/s
x_i	Mole fraction of component i in the liquid phase
y_i	Mole fraction of component i in the vapor phase
υ	Stoichiometric coefficient of the reaction
γ	Liquid phase activity coefficient
ξ	Dimensionless time

Subscripts

i	Component i
p	Product
r	Reactant

Acknowledgment

The authors acknowledge the financial support for this work from the National Natural Science Foundation of China (21376053), the Natural Science Foundation of Shandong Province, China (ZR2017QB006) and the Colleges and universities in Shandong Province science and technology projects (J16LC22).

Received : Jan 25, 2016 ; Accepted : Oct. 16, 2017

REFERENCES

[1] Li C.S., Daisuke H., Suzuki K., N-butyl Acetate Synthesis Via Reactive Distillation: Thermodynamic, Process Design, *Computers & Applied Chemistry*, **1124**: 1585-1589 (2009).

[2] Liao A.P., Tong Z.F., Synthesis of Butyl Acetate Catalyzed by Amberlyst, *Chemical Reaction Engineering & Technology*, **11**: 406-408 (1995).

[3] Arpornwichanop A., Koomsup K., Assabumrungrat S., Hybrid Reactive Distillation Systems for n-butyl Acetate Production from Dilute Acetic Acid, *Journal of Industrial & Engineering Chemistry*, **14**: 796-803 (2008).

[4] Hanika J., Kolena J.,Smejkal Q., Butyl Acetate *via* Reactive Distillation: Modelling and Experiment, *Chemical Engineering Science*, **54**: 5483-5490 (1999).

[5] Steinigeweg S., Gmehling J., n-Butyl Acetate Synthesis Via Reactive Distillation: Thermodynamic Aspects, Reaction Kinetics, Pilot-Plant Experiments, and Simulation Studies, *Industrial & Engineering Chemistry Research*, **41**: 5483-5490 (2002).

[6] Gangadwala J., Radulescu G., Kienle A., Sundmacher K., Computer Aided Design of Reactive Distillation Processes for the Treatment of Waste Waters Polluted with Acetic Acid, *Computers & Chemical Engineering*, **31**: 1535-1547 (2007).

[7] Jimenex L., Costa-Lopez J., The Production of Butyl Acetate and Methanol Via Reactive and Extractive Distillation. II Process Modeling, Dynamic Simulation, and Control Strategy, *Industrial & Engineering Chemistry Research*, **41**: 6735-6744 (2002).

[8] Jimenez L., Wanhschafft Q.M., Julka V., Analysis of Residue Curve Maps of Reactive and Extractive Distillation Units, *Computers & Chemical Engineering*, **25**: 635-642 (2001).

[9] Marcelino C.R., Juan G.S.H., Adrian B.P., A Short Method to Calculate Residue Curve Maps in Multireactive and Multicomponent Systems, *Industrial & Engineering Chemistry Research*, **50**: 2157-2166 (2011).

[10] Peters M., Kauchali S., Hildebrandt D., Glasser D., Application of Membrane Residue Curve Maps to Batch and Continuous Processes, *Industrial & Engineering Chemistry Research*, **47**: 2361-2376 (2008).

[11] Huang Y.S., Kai S., Schlünder E.U., Theoretical and Experimental Study on Residue Curve Maps of Propyl Acetate Synthesis Reaction, *Chemical Engineering Science*, **60**: 3363-3371 (2005).

[12] Sánchez-Daza O., Escobar G.V., Zárate E.M., Muñoz E.O., Reactive Residue Curve Maps a New Study Case, *Chemical Engineering Journal*, **117**: 123-129 (2006).

[13] Almeida-Rivera C.P., Swinkels P.L.J., Grievink J., Designing Reactive Distillation Processes: Present and Future, *Computers & Chemical Engineering*, **28**: 1997-2020 (2004).

[14] Duarteet C., Loureiro J.M., Effect of Adsorption on Residue Curve Maps for Heterogeneous Catalytic Distillation Systems, *Industrial & Engineering Chemistry Research*, **43**: 3242-3250 (2004).

[15] Zheng H.D., Tian H., Zou W.H., Huang Z.X., Residue Curve Maps of n-butyl Acetate Synthesis Reaction, *Journal of Central South University of Technology*, **20**: 50-56 (2013).

[16] Wang X.D., Wang Q.L., Ye C.S., Dong X.L., Qiu T., Feasibility Study of Reactive Distillation for the Production of Propylene Glycol Monomethyl Ether Acetate Through Transesterification, *Industrial & Engineering Chemistry Research*, **56**: 7149-7159 (2017).

[17] José S.L.V., Izabela D.G., Miguel Á.G.G., Vapour-Liquid Equilibrium and Distillation Scheme for the Hydrochloric Acid-Ethanol-Water Ternary Mixture, *Canadian Journal of Chemical Engineering*, **94**: 2380-2385 (2016).

[18] You X.Q., Gu J.L., Peng C.J., Shen W.F., Liu H.L., Improved Design and Optimization for Separating Azeotropes with Heavy Component as Distillate through Energy-Saving Extractive Distillation by Varying Pressure, *Industrial & Engineering Chemistry Research*, **56**: 9156-9166 (2017).

[19] Thakur S.S., Ojasvi Kumar V., Kaistha N., Continuous Diisobutylene Manufacturing: Conceptual Process Design and Plantwide Control, *Computers & Chemical Engineering*, **97**: 59-75 (2017).

[20] Dacruz F.E., Manousiouthakis V.I., Process Intensification of Reactive Separator Networks Through the IDEAS Conceptual Framework, *Computers & Chemical Engineering*, **105**: 39-55 (2017).

[21] Sorbier L., Bazer-Bachi F., Moreaud M., Moizan-Basle V., Mean Penetration Depth of Metals in Hydrodemetallation Catalysts, *Chemical Engineering Science*, **155**: 186-193 (2016).

[22] Mizzi B., Meyer M., Prat L., Augier F., Leinekugel-Le-Cocq D., General Design Methodology for Reactive Liquid-Liquid Extraction: Application to Dicarboxylic Acid Recovery in Fermentation Broth, *Chemical Engineering and Processing*, **113**: 20-34 (2017).

[23] Qiu T., Huang Z.X., Cheng C.B., Wu Y.X., Kinetics of Synthesis n-butyl Acetate over Cation-Exchange Resin Catalyst, *Chemical Reaction Engineering & Technology*, 25: 355-359 (2009).

[24] Elan G., "Aspen Plus User Guide, Version 10.2.California, Aspen Technology (1998).

[25] Cheng N.L., "Handbook of Solvents", Chemical Industry, Beijing (2007).

[26] Lee H.Y., Huang H.P., Chien I.L., Control of Reactive Distillation Process for Production of Ethyl Acetate, *Journal of Process Control*, **17**: 363-377 (2007).

[27] Zheng H.D., Lin M.M., Qiu T., Shen Y.Y., Tian H.; Zhao S.Y., Simulation Study of Direct Hydration of Cyclohexene to Cyclohexanol Using Isophorone as Cosolvent, *Chemical Engineering Research & Design*, **117**: 346-354 (2017).

[28] Xu Y., Ng F.T.T., Rempel G.L., Comparison of a Pseudo-homogeneous Nonequilibrium Dynamic Model and a Three-phase Nonequilibrium Dynamic Model for Catalytic Distillation, *Industrial & Engineering Chemistry Research*, **44**: 6171-6180 (2005).

[29] Tian H., Zheng H.D., Huang ZH.X., Qiu T., Wu Y.X., Novel Procedure for co-Production of Ethyl Acetate and n-Butyl Acetate by Reactive Distillation, *Industrial & Engineering Chemistry Research*, **51**: 5535-5541 (2012).